Probabilistic Engineering Mechanics 73 (2023) 103451

Contents lists available at ScienceDirect

Probabilistic Engineering Mechanics

journal homepage: www.elsevier.com/locate/probengmech

A procedure to estimate the Minimum Observable Damage in truss structures using vibration-based Structural Health Monitoring systems

Milad Jahangiri [a,b], Antonio Palermo [b], Soroosh Kamali [a,b], Mohammad Ali Hadianfard [a], Alessandro Marzani [b,*]

[a] Department of Civil and Environmental Engineering, Shiraz University of Technology, Modarres Blvd., Shiraz, 71557-13876, Fars, Iran
[b] Department of Civil, Chemical, Environmental and Materials Engineering, University of Bologna, Viale del Risorgimento 2, Bologna, 40136, Bo, Italy

ARTICLE INFO

Keywords:
Minimum observable damage
Uncertain modal data
Structural damage detection
Receiver Operating Characteristic
Vibration based SHM

ABSTRACT

In this work, we propose a procedure to estimate the Minimum Observable Damage (MOD) by a vibration-based Structural Health Monitoring (SHM) system. The MOD is defined as the smallest damage size that can be detected by an SHM system with given Probability of Detection (POD) and Probability of False Alarm (PFA). To this purpose, the MOD is computed by exploiting the Receiver Operating Characteristic (ROC) analysis, once a damage index (DI) built on monitoring data/features is defined. In particular, the MOD is defined as the damage intensity corresponding to an area under the ROC curve of 95%. The proposed idea is discussed by utilizing pseudo-experimental data generated via numerical simulations for undamaged and damaged structures. In the developed simulations, environmental uncertainties and measurement noises are considered. As case studies, we consider truss structures and use modal data, namely frequencies of vibrations and mode shapes, to build the DIs. Using the dataset of DIs, the ROC methodology is exploited to establish the probability of detecting certain damage over the probability of false alarms. For a given DI, results are provided in terms of MOD for each structural element of the truss structure considering one damaged element at a time. By establishing a relation between modal data, damage size, and POD/PFA, the proposed approach can assess the quality of the adopted DI, thus supporting the initial design of an SHM system.

1. Introduction

Vibration-based structural health monitoring (SHM) aims at the detection of damages, namely mechanical or geometrical changes of structural elements, by exploiting modal parameters (i.e., modal frequencies, mode shapes, and modal damping) [1–3]. To this purpose, accelerations due to ambient vibrations are recorded in several locations along the structure and modal parameters are estimated via Operational Modal Analysis procedures [4,5]. Such parameters are then used to feed metrics, commonly termed as damage indexes (DIs), meant at denoting the appearance, and eventually the evolution, of structural damages [1–3].

In this context, one of the main issues is the limited number and accuracy of modal parameters that can be experimentally estimated from the monitored accelerations due to the low levels of excitation, as well as due to the presence of environmental uncertainties and measurement noises [6,7]. Among the environmental uncertainties, for instance, the temperature is acknowledged as the main source of variability in the modal parameters due to its effect on structural parameters and boundary conditions [8–12]. Similarly, measurement noises along the data acquisition chain and/or induced by the operational conditions (e.g., traffic), can impact the number and accuracy of modal data that can be estimated from recorded accelerations, thus limiting the potential of SHM systems.

To overcome these limitations, SHM systems generally rely on (i) an increased number of sensors, (ii) sensors with higher sensitivity, (iii) measuring chains with higher performance, and (iv) advanced signal processing strategies. Still, these countermeasures introduce additional costs and complexities in the SHM system and thus their adoption should be carefully evaluated.

Motivated by this need, here we propose a procedure to quantify the minimum level of detectable damage in a structure for a given number of modal parameters exploited by a vibration-based SHM system.

First, we introduce the concept of Minimum Observable Damage, namely the smallest damage intensity characterized by a high Probability of Detection (POD) and low Probability of False Alarm (PFA) that can be detected for a given damage index (DI) built on a set of modal parameters. To this aim, we compute the distribution of the DI for the healthy structure (the baseline), where temperature and added noise introduce variability on the modal parameters and, in turn, on the DI. Similarly, we compute the distribution of the DI of the damaged structure for a certain level of the damage κ_i.

* Corresponding author.
E-mail address: alessandro.marzani@unibo.it (A. Marzani).

https://doi.org/10.1016/j.probengmech.2023.103451
Received 15 January 2023; Received in revised form 19 March 2023; Accepted 30 March 2023
Available online 11 April 2023

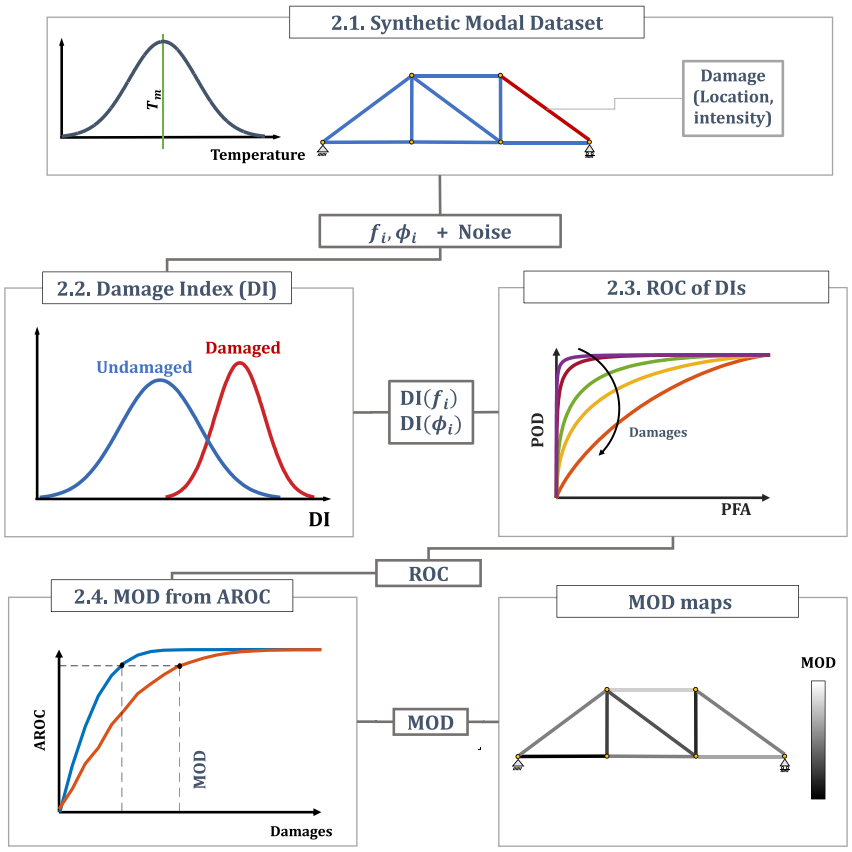

Fig. 1. Flowchart of the proposed method.

Using the DI distributions of the baseline and damaged structure, we compute the Receiver Operating Characteristic (ROC) curve [13,14] and evaluate the Area under the ROC curve (AROC). The AROC measures the accuracy of the considered DI in discriminating the κ_i damaged scenario from the healthy one with respect to a random classifier. We replicate the procedure by increasing the damage size in order to obtain a relationship between the AROC and the damage size. We finally define the Minimum Observable Damage (MOD) as the damage level associated to an AROC of 95% so that the MOD is characterized by a high POD and a low PFA.

Overall, the procedure allows assessing the performance of the vibration-based SHM approach for each damaged scenario, namely the values of MOD versus the damage index considered, and thus versus the number and type of modal data exploited.

To discuss the proposed methodology, we consider truss structures and build synthetic datasets of modal data using a standard finite element model. The datasets are built by considering a single damaged element of a truss structure at a time. To account for environmental and operational variability, all the numerical examples include the effect of temperature variation and measurement noises on the modal parameters. To this end, normally [15,16] and uniformly [17–19] distributed random noises are respectively applied to the elastic modulus of the elements and the computed modal data. The DIs are computed by exploiting classical damage metrics like the Natural Frequency Ratio (NFR) [20,21] and the Modal Assurance Criterion (MAC).

A two-dimensional statically determinate truss bridge, a two-dimensional truss tower with an increasing level of structural redundancy, and a three-dimensional redundant tower, are used to discuss the proposed methodology.

The work is organized as follows. First, the methodology is described in Section 2. A first application on simple statically determined truss structure is shown in Section 3. The suitability and performance of the proposed procedure are investigated on different truss structures in Section 4. Finally, some conclusions and perspectives are provided at the end of the work.

2. Proposed methodology

In this section, we briefly describe the approach to simulate the modal parameters of truss structures considering the influence of temperature variations and measurement noise. The distributions of modal parameters, computed for both healthy and damaged structures, are exploited to build distributions of damage indexes DIs. In particular, damage indicators like the NFR and the MAC, computed from natural frequencies and mode shapes, respectively, are used to define the DIs. Next, ROC curves computed on the DI distributions are used to correlate the number and type of modal parameters to the minimum observable damage in each element of the truss structure. The procedure is schematically summarized in Fig. 1 and described in the section.

2.1. Pseudo modal datasets

Truss structures are modeled via the finite element method where each ith truss element of the structure is characterized by Young's modulus E_i and cross-section A_i. In order to simulate modal parameters with a given variability, first a temperature-dependent Young's modulus is considered in the formulation of the dynamic equilibrium equations, and later the computed modal parameters are polluted by noise. The temperature-dependent Young's modulus is $E_i(T_i) = E^0\left[1-\beta(T_i-T_0)\right]$, where E^0 is the nominal modulus at the reference temperature T_0, β is the linear regression coefficient, and where the temperature T_i is sampled from a normal distribution centered at T_0 and having a standard deviation of σ_T [8–12].

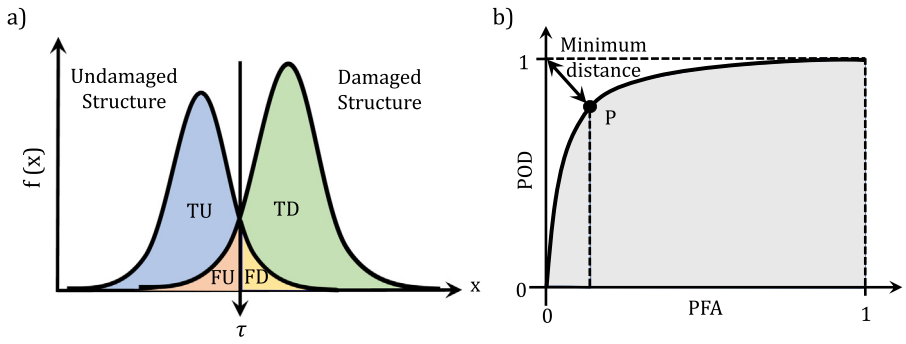

Fig. 2. (a) Bi-variate classification for two independent distributions; (b) receiver operating characteristic (ROC) curve.

For each T_i, the modal parameters of the structure are computed by finding the eigensolutions of the dynamic equilibrium equation [22,23]:

$$[\mathbf{K}_e + \mathbf{K}_g - \omega_j^2 \mathbf{M}]\phi_j = \mathbf{0} \tag{1}$$

where the global elastic stiffness matrix $\mathbf{K}_e$, geometric stiffness matrix $\mathbf{K}_g$, and mass matrix $\mathbf{M}$, are considered. Note that the linearized geometric stiffness matrix $\mathbf{K}_g$ depends on the internal axial forces induced by the equivalent thermal nodal loads and is not null in redundant truss structures. In Eq. (1), $\omega_j = 2\pi f_j$ and ϕ_j are the jth natural frequency and mode shape of the structure, respectively.

A scenario is defined by setting a damage level in a given element of the truss. In particular, damage scenarios where a single element is damaged are considered. The damage in the ith element is modeled as a reduction of its axial stiffness $E_i A_i$, herein denoted as *damage size*, as:

$$\kappa_i = 1 - \frac{E_i^d A_i^d}{E_i^u A_i^u} \tag{2}$$

where u and d refer to undamaged and damaged scenarios, respectively, with $\kappa_i \in [0 - 1]$. It follows that $\kappa_2 = 0.1$, for example, denotes a reduction of the axial stiffness in the element number 2 of 10%.

For a given scenario, we perform N numerical simulations to build a dataset of modal solutions affected by the variability induced by the temperature T_i. Additionally, to account for noise typically encountered along the measurement chain, the modal parameters are polluted as follows [17–19,24,25]:

$$\tilde{f}_j = f_j \left[1 + n_f(2p - 1)\right] \tag{3}$$

$$\tilde{\phi}_j(l) = \phi_j(l) \left[1 + n_{\Phi}(2p - 1)\right] \tag{4}$$

where $\tilde{f}_j$ is the jth natural frequency polluted by noise, n_f is the level of noise of the natural frequency, and p is sampled from a uniform distribution, i.e., $p \in [0-1]$. Similarly, $\tilde{\phi}_j(l)$ is the lth component of the jth mode shape and n_ϕ the level of noise applied to the mode shapes. In this example, values of $n_f = n_\phi = 1\%$ are considered.

2.2. Damage index (DI)

From the set of modal parameters associated to a damage size κ_i, the Natural Frequency Ratio (NFR) [20,21] and the Modal Assurance Criterion (MAC) [20,21], are built as follows:

$$NFR_j = \frac{\tilde{f}_j}{\tilde{f}_j^r} \tag{5}$$

$$MAC_j = \frac{|\tilde{\phi}_j^{r^T} \tilde{\phi}_j|^2}{(\tilde{\phi}_j^{r^T} \tilde{\phi}_j^r)(\tilde{\phi}_j^T \tilde{\phi}_j)} \tag{6}$$

where $\tilde{f}_j^r$ is the reference jth frequency, computed as the mean of all the N frequencies $\tilde{f}_j$ for the undamaged structure. Likewise, $\tilde{\phi}_j^r$ is the reference mode shape, namely the mean value of all N mode shapes of the undamaged structure.

Based on the damage indicators of Eqs. (5) and (6), two damage indices are built as:

$$DI = 1 - \frac{1}{m} \sum_j NFR_j \tag{7}$$

$$DI = 1 - \frac{1}{m} \sum_j MAC_j \tag{8}$$

with m being the number of modal parameters used in the DI computation. For instance, if $j = [1, 3, 5]$, the first, third and fifth frequencies or mode shapes are used, with $m = 3$. Other DIs, based on the combination of frequencies and mode shapes, could be easily considered. Still, the scope of this work is not towards the identification of the best DI for the considered structures but more on proposing a procedure to estimate the MOD. Indeed, the proposed procedure could be also applied to static monitoring parameters as well as to a combination of static and dynamic monitoring parameters, as long as they can be considered to form a DI.

2.3. DI performance via ROC curves

We use the Receiver Operating Characteristic (ROC) curve [26] to quantify the ability of a certain damage index (DI) to properly classify undamaged versus damaged scenarios. For each scenario, we consider two distributions of DI, one with N samples computed for the undamaged structure and a second one with N samples computed for the damaged one (see Fig. 2a). Given this dataset, a threshold τ on the DI is defined to label each sample as undamaged, when DI $< \tau$, or damaged when DI $> \tau$, respectively. Depending on the chosen τ and the DI distributions, the obtained classification can be either correct (true) or incorrect (false). The classification performance of the DI for the given threshold can by computed by the number of:

- true undamaged (TU) samples, namely the number of undamaged samples correctly classified as undamaged;
- false undamaged (FU) samples, namely the number of damaged scenarios incorrectly classified as undamaged;
- true damaged (TD) samples, namely the number of damaged scenarios correctly classified as damaged;
- false damaged (FD) samples, namely the number of undamaged samples incorrectly classified as damaged.

In particular, for a given τ, the probability of detection $POD(\tau)$ and the probability of false alarm $PFA(\tau)$ can be defined as follows:

$$POD(\tau) = \frac{TD(\tau)}{TD(\tau) + FU(\tau)} \tag{9}$$

$$PFA(\tau) = \frac{FD(\tau)}{FD(\tau) + TU(\tau)} \tag{10}$$

or equivalently as:

$$POD(\tau) = \int_{\tau}^{+\infty} f_d(x)dx = 1 - F_d(\tau) \tag{11}$$

$$PFA(\tau) = \int_{\tau}^{+\infty} f_u(x)dx = 1 - F_u(\tau) \tag{12}$$

when the probability density functions $f_d(x)$ and $f_u(x)$ and the cumulative distribution functions $F_d(\tau)$ and $F_u(\tau)$ are known. It is worth mentioning that Eqs. (9) and (10) are applicable to discrete variables, whereas Eqs. (11) and (12) represent their extension to continuous variables. In Eq. (9), $TD(\tau)$ is the number of damaged DIs greater than τ, and $TD + FU$ is the total number of damaged DIs. Therefore, $TD/(TD + FU)$ represents the probability that a random DI is greater than τ. Similarly, Eq. (11), namely the integral from τ to $+\infty$ of the probability density function, is equivalent to $P(x > \tau)$, where the variable x is a sample of the DI distribution. Analogous considerations can be made for Eqs. (10) and (12).

The ROC curve is thus obtained by plotting the $POD(\tau)$ vs $PFA(\tau)$, see Fig. 2b. Given the $POD(\tau)$ vs. $PFA(\tau)$ relationship, the Area under the ROC curve can be computed as:

$$AROC = \int_0^1 POD(PFA^{-1}(x))dx \tag{13}$$

where x is the PFA, and $PFA^{-1}(x)$ is the threshold value τ that must be provided to obtain that PFA (i.e., its argument).

The AROC provides the probability that the given classifier, i.e., the DI, ranks a randomly chosen damaged instance higher than a randomly chosen undamaged instance. A more intuitive explanation of its value can be found by looking at the ROC representation in Fig. 2(b). For a ROC curve, in fact, it is possible to identify a so-called optimal point P, having a minimal distance w.r.t a perfect classifier with $POD = 1$ and $PFA = 0$, namely no damages missed with zero false alarms. Note that when P approaches the condition $POD = 1$, $PFA = 0$, the AROC approaches the unit value. More in general, a large value of AROC is associated with an optimal point with high POD and low PFA, a desirable condition for any DI.

2.4. Minimum observable damage from AROC curves

For a given selected element of the structure, namely the ith element, we compute the AROC for $\kappa_i = [0.0, 0.1, 0.2, 0.3, \dots, 1.0]$ and build the curve AROC versus size of damage. As an example, in Fig. 3, three AROC versus damage curves are shown. These curves are not computed from dataset of a specific structure but are artificially built to clarify the MOD computation approach. To this end, we consider normal distributions of $N = 5000$ samples, each having a mean equal to κ_i ($0 \le \kappa_i \le 1$) and standard deviation σ equal to 10%, 20% and 30% of κ_i. The case with $\kappa_i = 0$ is the one representative of the undamaged scenario (baseline). Non-zero values of κ_i refer, instead, to damaged scenarios. We exploit the AROC curve to estimate the minimum observable damage in the ith element of the truss. In particular, we set the MOD as the damage intensity related to an AROC value of 95%. As such the MOD for the scenario κ_i considering $\sigma = 10\%$, $\sigma = 20\%$ and $\sigma = 30\%$ are equal to 0.24, 0.46 and 0.70, respectively.

In practical cases, as it will be shown in the next section, for the same modal properties considered, different DIs will lead to different AROC curves and thus to different MOD for the same AROC value of 95%. As such, the proposed strategy allows to formulate the best DI by relating the considered modal properties to the structural damage.

3. Numerical application

We consider the 9-bar planar truss structure shown in Fig. 4. The truss is composed of steel bars with nominal $E^0 = 200$ GPa, temperature correlation coefficient β=0.0036%, reference temperature $T_0 = 20$ °C. For each element, mass density of $\rho = 7850$ kg/m^3, cross-sectional area

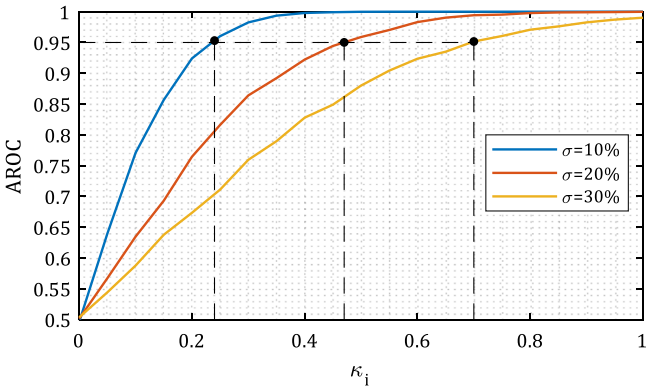

Fig. 3. Artificially built AROC vs damage curves.

of $A = 0.0025$ m^2, and thermal expansion coefficient $\alpha = 1.17\times10^{-5}$, are considered. The temperature T_i is sampled from a normal distribution with standard deviation of $\delta_T = 1$ °C centered at T_0. As an example, we show in Fig. 5 the distributions of the NFR and MAC for the first three frequencies and modes shapes, $j = 1, 2, 3$, obtained by $N = 100$ simulations for the undamaged $\kappa_2 = 0$ (blue) and $N = 100$ simulations for damaged $\kappa_2 = 0.1$ (yellow) scenarios.

We exploit the proposed procedure to estimate the minimum observable damage in the element number 2 of the truss. To this purpose, for $\kappa_2 = [0, 0.01, 0.02, \dots, 0.3]$, we compute for each damage size the modal properties, different damage indexes and the related AROC curves. In particular, in Fig. 6a we show the variation of five different damage indexes, namely $DI_1(f_1)$, $DI_2(f_2)$, $DI_3(f_3)$, $DI_4(f_1, f_2)$ and $DI_5(f_1, f_2, f_3)$, with respect to the damage size κ_2, where for example $DI_4(f_1, f_2)$ denotes the DI computed by considering Eq. (7) and the first two frequencies f_1 and f_2. Since for each damage level N=100 samples are computed, the mean value and the standard deviation of the DIs, namely $\mu(DI)$ and $\sigma(DI)$, are represented in Fig. 6a and b, respectively. Finally the AROC curves are shown in Fig. 6c. As expected, the AROC for all the computed DIs increases by increasing the damage size. Similarly, the use of a larger number of frequencies is beneficial to improve the classification performance of the DI measured by the AROC. We remark that the non-smooth behavior of the AROC curves is due to the finite sampled space of instances, $N = 100$ in this case, considered to built the DI distributions.

We define the damage size related to AROC=0.95 as the minimum observable damage for the given truss element. Since this damage size is related to an AROC=0.95, its optimal point is associated with a high POD and a low PFA, as discussed in the previous section.

In this regard, the MOD computed for DIs based simply on the 1st, 2nd, and 3rd natural frequencies, Fig. 6, c are equal to 18%, 11%, and 7%, respectively. In addition, the MOD for element 2 decreases to 8% and 6% considering a DI based on the combined first two and first three natural frequencies, respectively. In this regard, one can observe how the third frequency alone contributes mostly to reducing the minimum observable damage.

It should be noted that the plot of DI vs. κ does not retain information on the PFA and/or POD, whereas the AROC plot of Fig. 6c contains information on both parameters at the same time. We emphasize here that a larger DI does not necessarily represent a better damage index to use. For example, DI_3 in Fig. 6a is the largest index, whereas in Fig. 6c, DI_5 is more effective based on the AROC values. The reason is related to the higher standard deviation of DI_3 w.r.t. DI_5, as it can be seen in Fig. 6b. Such higher standard deviation reduces the values of the ROC curves for DI_3 and, in turn, its AROC curves. As such, the AROC curve does not only retain the information of PFA and POD but contemplates both the mean and standard deviation of the DI for damage detection purposes.

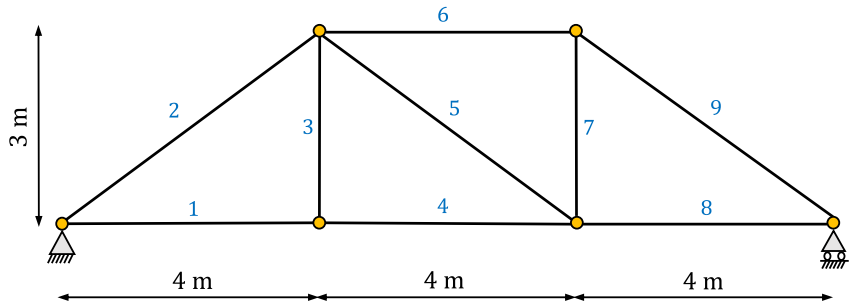

Fig. 4. Schematic of the 9-bar planar truss structure.

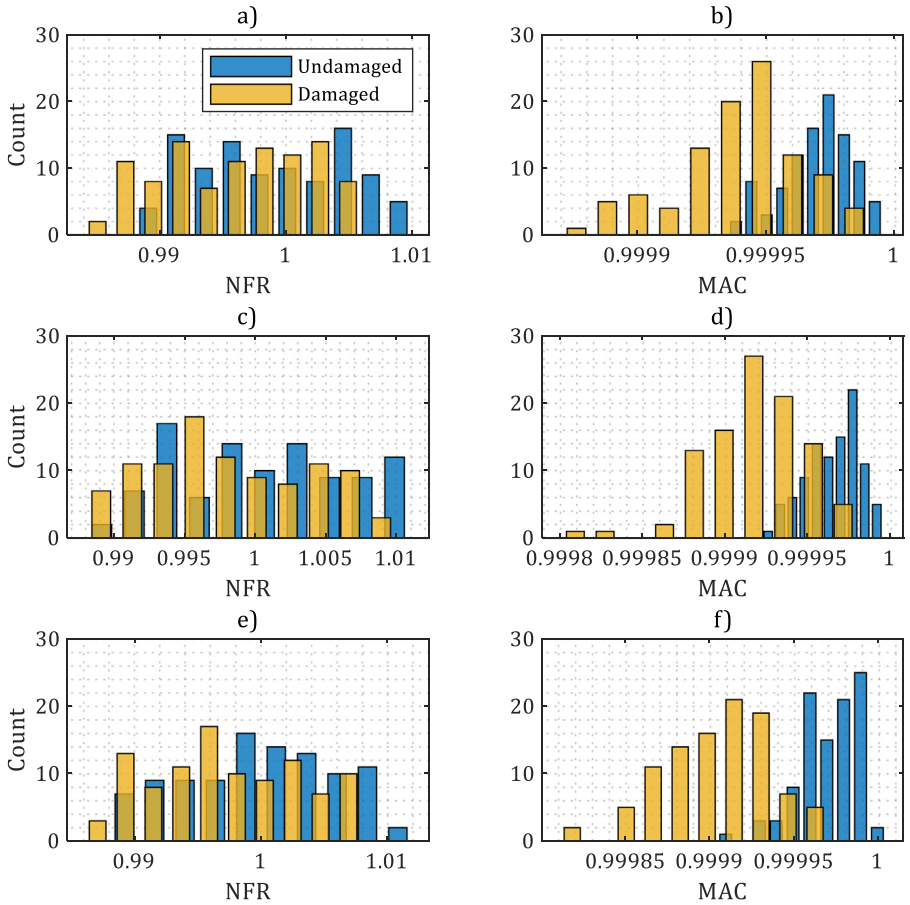

Fig. 5. NFR and MAC probability density functions for undamaged (blue) and damaged structure (yellow) considering $\kappa_2 = 0.1$: (a)–(c)-(e) first, second and third frequency; (b)–(d)-(f) first, second and third mode shape.

The same study can be extended to all the truss elements of the structure. In particular, in Fig. 7a we report the MOD computed for DIs based on the 1st, 2nd, and 3rd natural frequencies and the combination of all of them. The reader can appreciate how changing the DIs result in significantly different MOD results. Note that none of the DIs based on a single frequency can ensure a MOD $\kappa_i < 0.8$ for all the truss elements (see Fig. 7a). Additionally, regardless of the damage size, the DIs based on the 3rd natural frequency cannot identify damages in elements 1 and 4 with the desired AROC value, namely MOD=1 for DI_3 in Fig. 7a. The existence of such unobservable damages (UD) for an AROC value of 0.95 in a statically determinate structure can be particularly critical since unobservable damages would lead to the collapse of the structure. Overall, the use of multiple frequencies as in DI_5 (see Fig. 7a) improves the performance of the classifier, avoiding the presence of UDs, and yielding to a MOD $\kappa_i < 0.65$ in all the truss elements.

Similarly, in Fig. 7b we computed the MOD by considering the DIs built on MAC as per Eq. (8). In particular, Fig. 7b shows the MOD

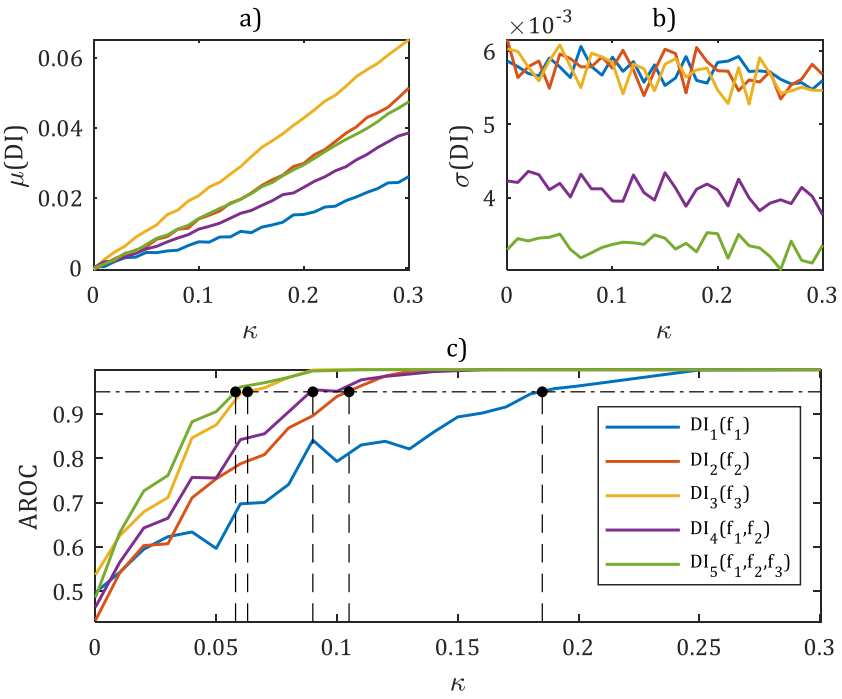

Fig. 6. Damage scenarios $\kappa_2 = [0, 0.01, \ldots, 0.3]$. (a) Damage indexes (DIs) mean value; (b) DIs standard deviation; (c) AROC curves for the different DIs.

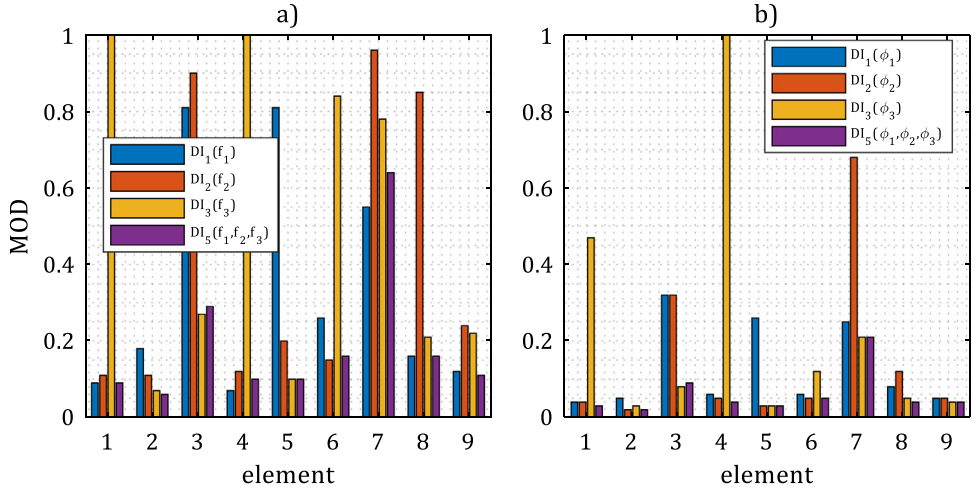

Fig. 7. MOD for a 9-bar planar truss structure considering (a) four damage indexes based on frequencies and (b) four damage indexes based on mode shapes. MOD equal to 1 denotes elements for which the MOD cannot be defined for AROC 95%.

computed by considering the first, second, and third mode shapes (ϕ_1, ϕ_2, and ϕ_3) and the combination of the three mode shapes.

As expected, a comparison between Fig. 7a and Fig. 7b highlights the superior performance of MAC-based DIs over NFR-based DIs. In particular, DIs based on the combination of the first three modes ensure a MOD $\kappa_i < 0.25$ for all the truss elements. Nonetheless, it must be remarked that all the components of the mode shapes have been used in the computation of the MAC. In practical scenarios, the components of a mode shape are estimated via Operational Modal Analysis (OMA) procedures only at those nodes and directions where an accelerometer is available. The other components are eventually estimated using modal expansion techniques which can introduce further uncertainties on the unmeasured components.

Besides this aspect, we observe how the use of different modal parameters yields significantly different MODs in the various elements of the structure. This variability reflects the sensitivity of the modal parameters to the location of the damages.

Next, we investigate the sensitivity of the MOD against the number of modal parameters used to compute the DIs accounting for the standard deviation δ_T used in input to generate the modal data. In this regard, Fig. 8 shows the MOD computed for an increasing number of frequencies and mode shapes for temperature standard deviations $\sigma_T = 1$ °C (first row), $\sigma_T = 5$ °C (second row), and $\sigma_T = 10$ °C (third row), respectively.

The MOD computed by considering the frequencies of vibration (Figs. 8a, b, c) reduces for all the elements of the structure by increasing the number of frequencies. For a DI computing with a number of frequencies equal to or larger than 6, the MOD for all the elements of the structure is approximately equal to 0.1, 0.2, and 0.3 for $\sigma_T = 1, 5, 10$ °C, as shown in Fig. 8a, b, c, respectively. Conversely, Figs. 8 d, e, f show that for DIs built on mode shapes, the best number of modes to consider is not nine, i.e. the maximum number of modes, but 4 or 5. By using 4 or 5 modes shapes the average MOD for all the elements of the structure is approximately 0.05, 0.1 and 0.2, for the cases of

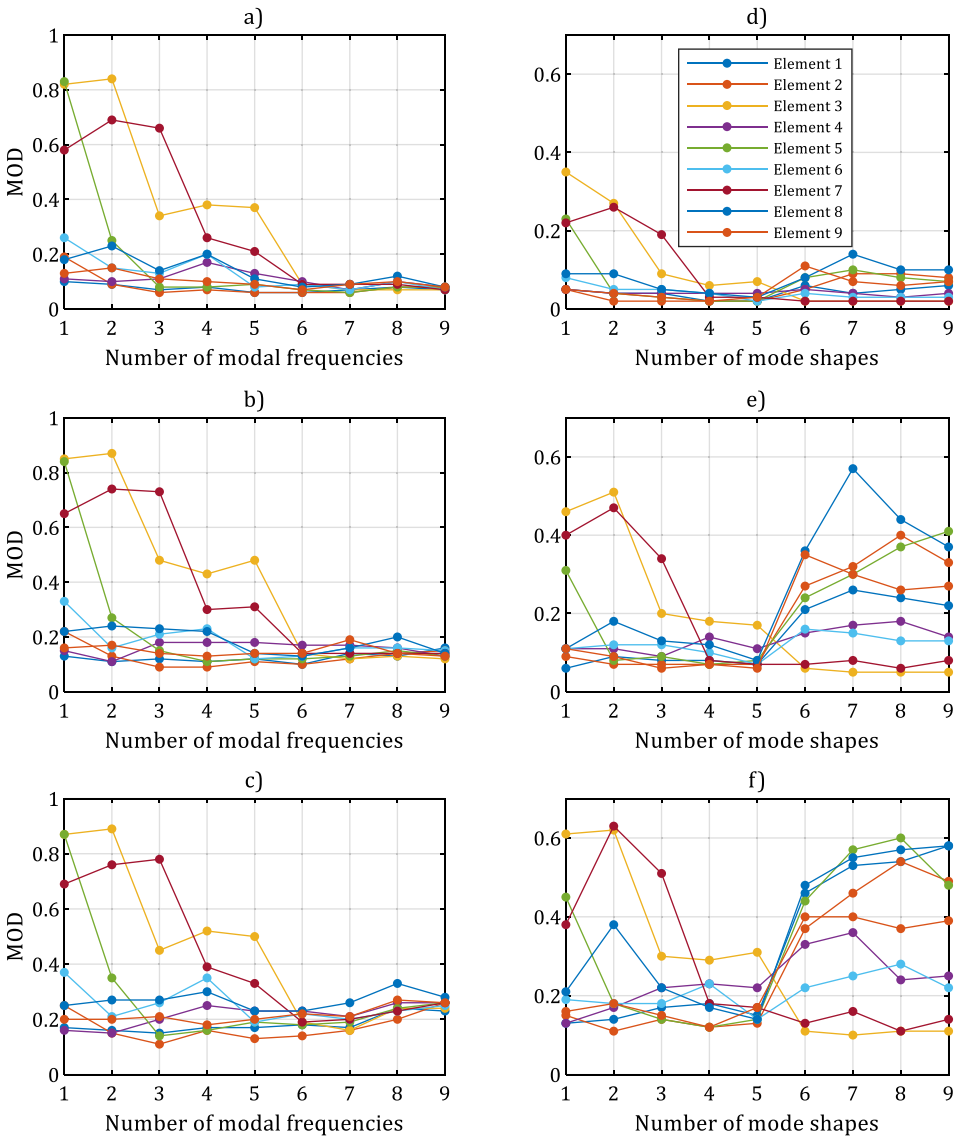

Fig. 8. MOD computed by considering NFR (left column) and MAC (right column) and a distribution of temperature having $\sigma_T = 1$ °C (first row), $\sigma_T = 5$ °C (second row), $\sigma_T = 10$ °C (third row).

$\sigma_T = 1, 5, 10$ °C. Hence, one can observe that, while for a small number of frequencies or modes, namely 1, 2 or 3, the use of modes w.r.t frequencies yields always a smaller MOD, the opposite takes place for DIs built by considering 6, 7, 8 or 9 frequencies or modes. As such, the proposed procedure helps in defining the best combination of modal parameters to be used in the DI computation.

To assess the reliability of the results discussed in Fig. 8, we perform statistical analysis on the MOD. In particular, considering distributions of DIs of $N = 30$ samples, i.e. obtained for 30 different values of temperature T_i, we computed the mean and the standard deviation of the MOD.

Fig. 9 shows that for each element and for the considered DI the standard deviation of the MOD (shaded area) is very low, thus confirming the reliability of the proposed procedure.

4. Case studies

In this section, we apply the procedure to three case studies and describe synthetically its outcomes in terms of MOD maps. These maps are obtained by reporting on the geometrical layout of the structure the MOD values for each element. As such, a MOD map gives clear and intuitive information on how different DIs can (or cannot) provide observable damage in any element of the structure.

4.1. Statically determinate 25-bar planar truss structure

Our first case study consists of the planar truss structure shown in Fig. 10. The structure has 25 elements and 14 nodes. All truss elements are characterized by material density 7850 kg/m^3 and Young's modulus 200 GPa at the reference temperature of 20 °C. The cross-section area of all vertical and top peripheral elements is 0.1164 m^2 whereas for all horizontal and diagonal elements is 0.0556 m^2. Concentrated loads of $P = 10$ kN are applied to the seven top nodes, in the vertical direction, and contribute to the generation of axial stresses in the elements and, in turn, to the magnitude of the geometric stiffness matrix.

The modal dataset accounts for N=100 samples (modal data) for each scenario, undamaged or damaged, with a $\sigma_T = 1$ and a noise level of 1% applied on the modal data.

The MOD maps computed for AROC values of 95% using NFR damage indicators to build the DIs are shown in Fig. 11. In particular,

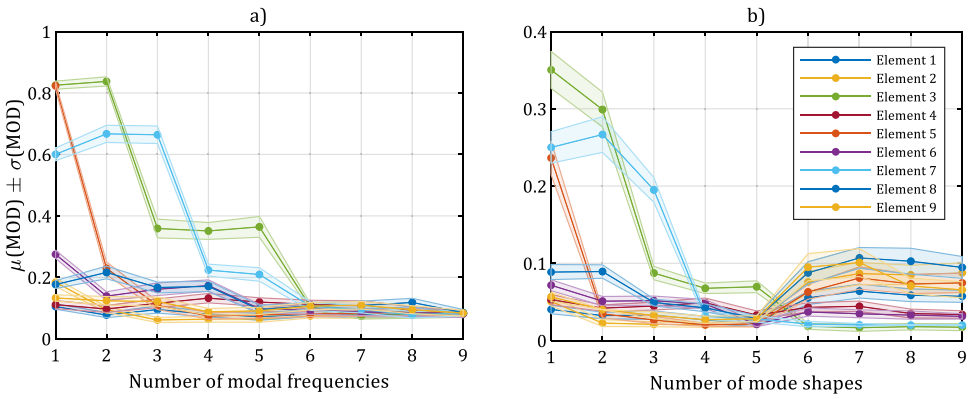

Fig. 9. (a) Sensitivity analysis of MOD vs. the number of frequencies considered to build the DI. (b) Sensitivity analysis of MOD vs. the number of mode shapes considered to build the DI.

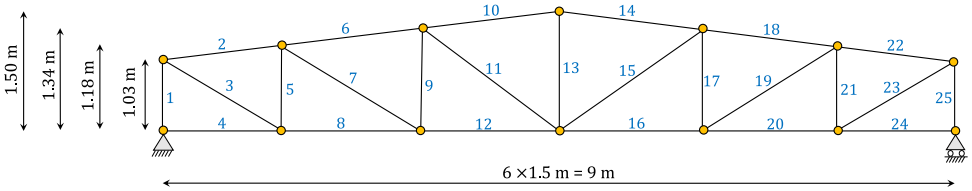

Fig. 10. A statically determinate 25-bar planar truss structure.

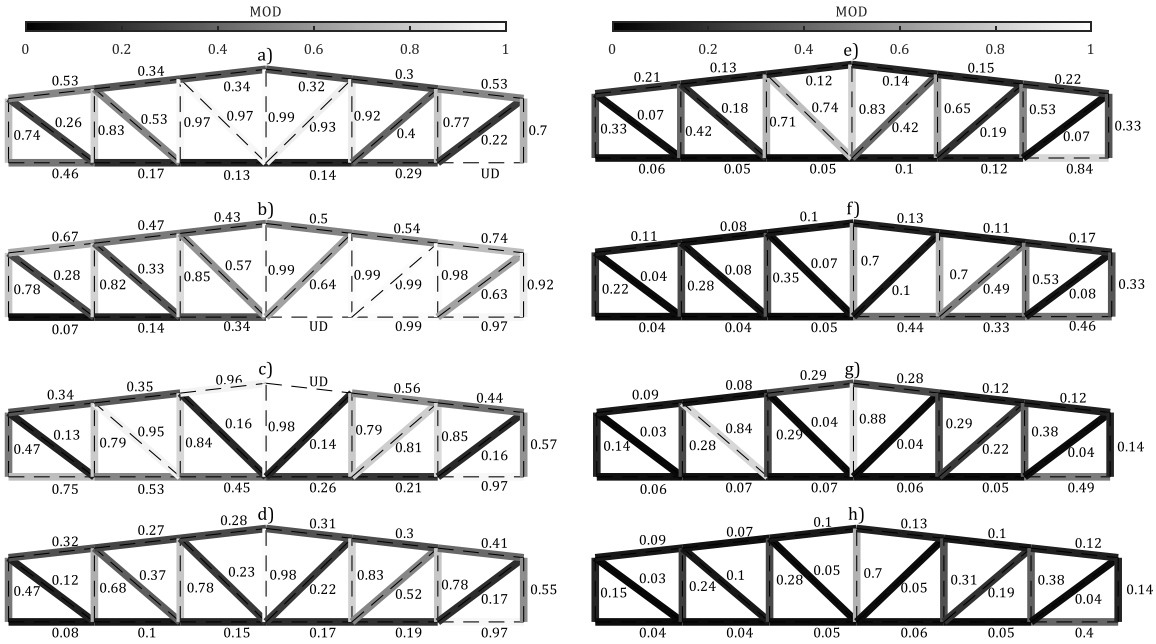

Fig. 11. MOD maps computed for (a) $DI_1(f_1)$; (b) $DI_2(f_2)$; (c) $DI_3(f_3)$; (d) $DI_5(f_1, f_2, f_3)$, (e) $DI_1(\phi_1)$; (f) $DI_2(\phi_2)$; (g) $DI_3(\phi_3)$; (h) $DI_5(\phi_1, \phi_2, \phi_3)$. UD denotes those elements with unobservable damage.

the MODs computed for $DI_1(f_1)$, $DI_2(f_2)$, $DI_3(f_3)$ and $DI_5(f_1, f_2, f_3)$, are shown in Fig. 11(a), (b), (c) and (d), respectively. For these plots, the average values of MOD are equal to 0.62, 0.71, 0.66, and 0.46, respectively. Nonetheless, elements with unobservable damages, namely MOD=1 or very close to that, are present for all the DIs considered, thus warning a possible SHM user of the blind spots of an SHM system using such common frequency-based DIs.

Alike, the MOD maps computed by considering MAC-based damage indexes are shown in the right column of Fig. 11. As expected, lower MODs indices are achieved using the MAC values of the first three mode shapes. In particular, the use of $DI_5(\phi_1, \phi_2, \phi_3)$ avoids the presence of unobservable damages (UD).

4.2. Structural redundancy vs the MOD

The approach is further discussed on a truss tower with increasing structural redundancy to examine its effect on the performance of the DIs and the related MODs. For this purpose, the planar truss structures shown in Fig. 12 are considered. They include a statically determinate truss (Fig. 12a), and three statically redundant trusses (Fig. 12b, c, d) with 1, 2, and 3 degrees of redundancy, respectively. All the structural members are made of steel with material density $\rho = 7850$ kg/m^3 and modulus of elasticity at a reference temperature of 20 °C of 200 GPa. The elements have an identical cross-sectional area $A = 0.1164$ m^2. Temperature effects and measurement noises are introduced

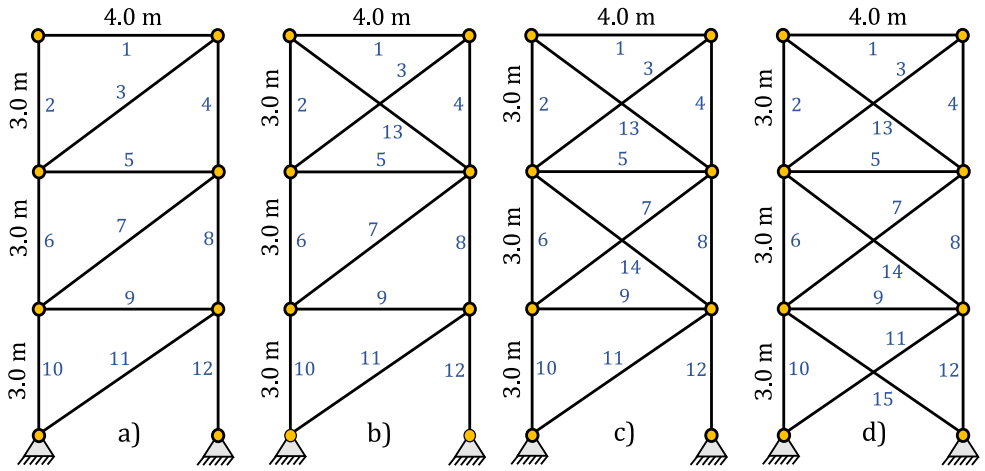

Fig. 12. The planar truss structures: (a) 12-bar; (b) 13-bar; (c) 14-bar; (d) 15-bar.

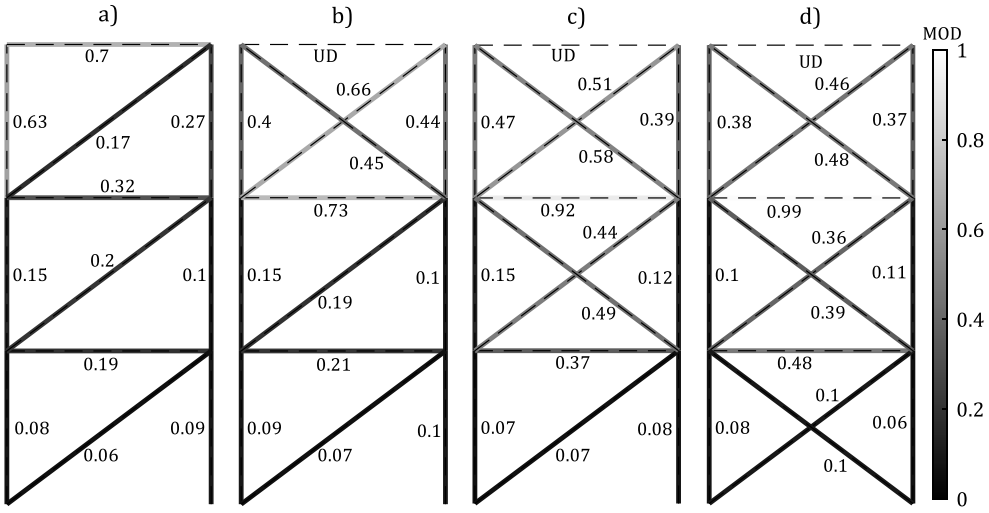

Fig. 13. MODs computed from the first three natural frequencies: (a) 12-; (b) 13-bar; (c) 14-bar; (d) 15-bar planar trusses.

as in the previous example. Alike, an AROC of 0.95 is assumed in the computation of the MOD.

Fig. 13 reports the value of the MOD obtained by considering the combination of the first three natural frequencies, namely $DI_5(f_1, f_2, f_3)$. For each structure, the MOD in the truss elements is minimum at the bottom level. Additionally, for the same class of elements, namely vertical, diagonal and horizontal bars, the MOD increases along the height of the tower, leading to unobservable damages at the top of the structure for the three statically redundant systems. Overall, the distribution of the MOD over the structures is in agreement with the distribution of modal strain energy associated with the modes of vibration considered in the DIs.

On average, the MOD increases when the degree of redundancy of the structure increases, e.g., the mean MOD computed by averaging the MOD of all the elements in the structure is 0.24, 0.36, 0.41, and 0.37, for the cases in Fig. 13(a), (b), (c) and (d), respectively.

The use of a MAC-based DI built on the combination of the first three mode shapes is able to partially mitigate this issue. In fact, from Fig. 14, where the MOD for the 4 structures is shown, we observe smaller values of MOD and smaller variations w.r.t. the structural redundancy. Indeed, the average values of MOD are equal to 0.09, 0.10, 0.12, and 0.10, for the structures in Figs. 14(a), 14(b), 14(c), and 14(d), respectively.

4.3. 3D tower

In this final example, we apply the proposed procedure to a three-dimensional 70-bar spatial truss structure. The length, width, and height of the structure are 1 m, 1 m, and 5 m, respectively, as shown in Fig. 15a. All the truss elements are characterized by circular hollow cross-section with external and internal diameters equal to 0.042 m and 0.036 m, respectively. The structure is restrained at the four bottom joints. The modulus of elasticity of the material at the reference temperature of 20 °C is $E = 70$ GPa and the mass density is 3129.86 $\mathrm{kg/m^3}$.

MODs are computed considering N=100 cases for the undamaged and damaged structures, $\sigma_T = 1$ °C, an added noise level on the modal parameters of 1%, and an AROC=0.95. Results are given in Fig. 15(b) and (c) in terms of colormaps of MOD ranging from 0 to 1. In particular MOD maps in Fig. 15(b) and (c) are computed for $DI_1(f_1)$ and $DI_5(f_1, f_2, f_3)$, respectively.

Alike for the 2D truss tower, the MOD decreases moving from the bottom of the structure to its top elements. The average values of MOD

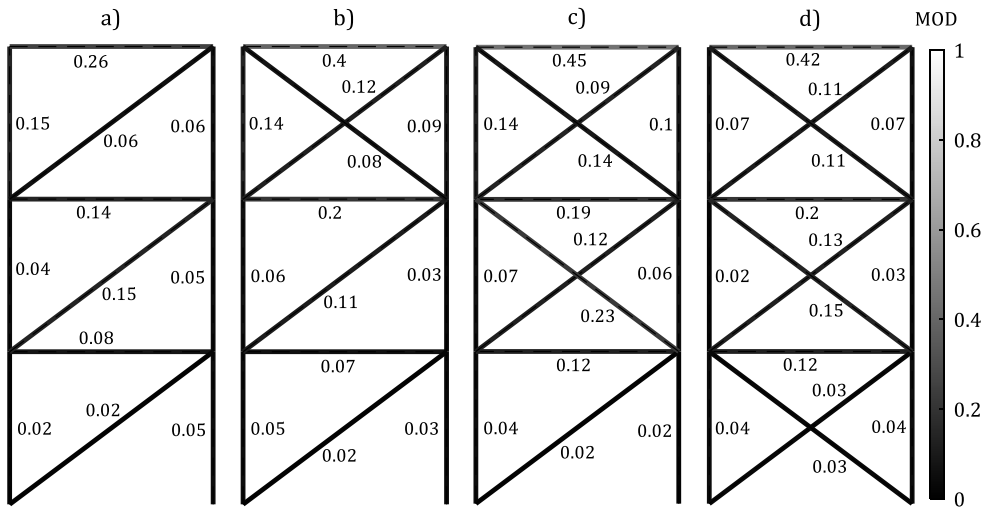

Fig. 14. MOD computed for the first three mode shapes: (a) 12-bar; (b) 13-bar; (c) 14-bar; (d) 15-bar planar trusses (UD represents the unobservable damages).

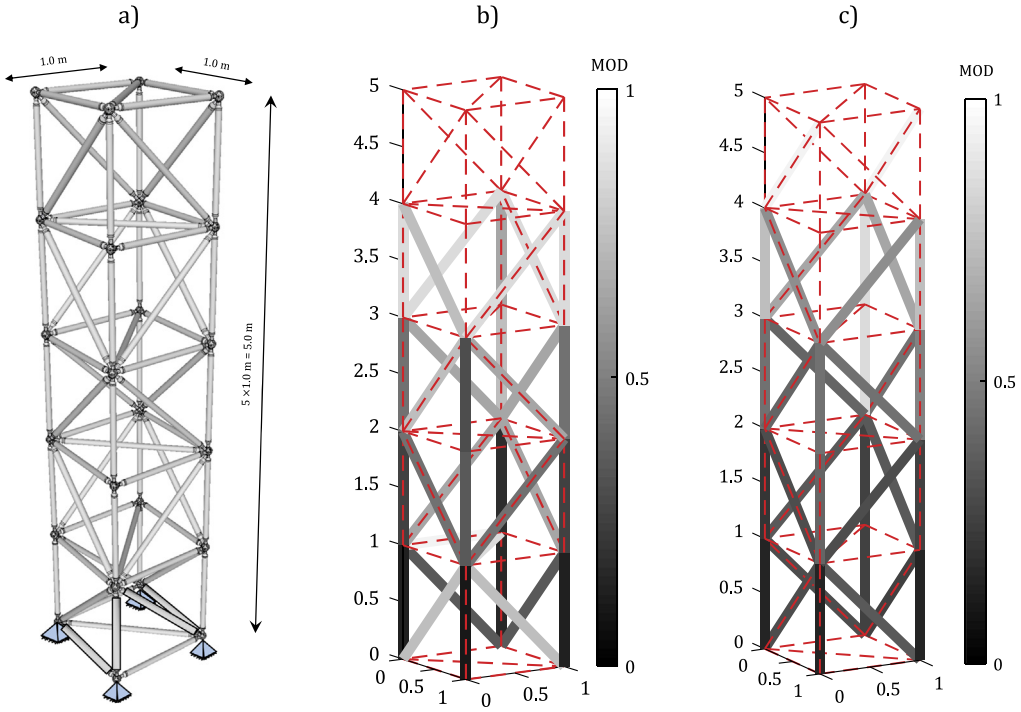

Fig. 15. (a) 3D truss structure. (b) MOD map computed for $DI_1(f_1)$. (c) MOD map computed for $DI_5(f_1, f_2, f_3)$.

in Fig. 15(b) and (c) are equal to 0.83 and 0.78, respectively. Although increasing the number of frequencies from one to three slightly improves the results, damages in many elements are still unobservable with the desired POD and PFA (namely AROC=0.95).

5. Conclusions

A procedure based on the use of the Receiver Operating Characteristic (ROC) has been proposed to introduce and estimate the minimum observable damage in truss structures, namely an element damage intensity that can be observed with a high POD and low PFA. For such purpose, a FE code has been used to generate synthetic datasets of modal data for healthy and damaged truss structures. Pseudo-modal data have been computed considering temperature variations in the structural element and adding measurement noises. Undamaged and damaged pseudo-modal data have been used to build damage indexes, later used to feed the ROC curves. ROC curves have been computed for increasing levels of damage, and the related AROC values have been used to estimate the MOD in the truss elements.

The proposed approach can provide a map that relates the considered modal parameters and the designed damage indicator to the minimum observable damage. We remark that one limitation of the results presented in this work is the consideration of damage scenarios where only a single element at a time is damaged. This choice was useful to plot the minimum observable damage maps. Still, the procedure is not limited to these damage scenarios, and can equivalently deal with cases where multiple elements of the structure are damaged.

In addition, we remark that the proposed method is here tested using simulated data rather than real measurements. This choice was dictated by the possibility of building multiple damage scenarios, more than those generally available from real data, to show the potential of the approach. Still, the simulated data considered are a reasonable representation of real data, as the added levels of noise on modal data

are those generally experienced by vibration-based monitoring systems. Overall, given its simplicity, the method can be used in the initial design phase of vibration-based SHM systems to estimate the number of modal parameters required to detect the presence of structural damage in an element with high POD and low PFA.

Funding

The authors did not receive support from any organization for the submitted work.

Code availability

Codes are available upon request.

CRediT authorship contribution statement

Milad Jahangiri: Conceptualization, Data curation, Methodology, Visualization, Writing – original draft. **Antonio Palermo:** Methodology, Supervision, Validation, Writing – review & editing. **Soroosh Kamali:** Methodology, Visualization, Validation, Writing – review & editing. **Mohammad Ali Hadianfard:** Methodology, Supervision, Writing – review & editing. **Alessandro Marzani:** Methodology, Supervision, Validation, Writing – review & editing.

Declaration of competing interest

The authors declare that they have no known competing financial interests or personal relationships that could have appeared to influence the work reported in this paper.

Data availability

Data will be made available on request.

References

[1] R. Perera, A. Ruiz, C. Manzano, An evolutionary multiobjective framework for structural damage localization and quantification, Eng. Struct. 29 (10) (2007) 2540–2550.
[2] R. Perera, R. Marin, A. Ruiz, Static–dynamic multi-scale structural damage identification in a multi-objective framework, J. Sound Vib. 332 (6) (2013) 1484–1500.
[3] R. Perera, A. Ruiz, C. Manzano, Performance assessment of multicriteria damage identification genetic algorithms, Comput. Struct. 87 (1–2) (2009) 120–127.
[4] M.A. Hadianfard, S. Kamali, Ambinet Vibrations: Measurement, Process, and Applications in Civil Engineering, Regional Information Center For Science and Technology, 2019.
[5] M.A. Hadianfard, S. Kamali, Analysis of modal frequencies estimated from frequency domain decomposition method, Int. J. Eng. Technol. 12 (3) (2020).
[6] C. Rainieri, G. Fabbrocino, Operational Modal Analysis of Civil Engineering Structures, 142, Springer, New York, 2014, p. 143.
[7] R. Brincker, C. Ventura, Introduction To Operational Modal Analysis, John Wiley & Sons, 2015.
[8] A.-M. Yan, G. Kerschen, P. De Boe, J.-C. Golinval, Structural damage diagnosis under varying environmental conditions—part I: a linear analysis, Mech. Syst. Signal Process. 19 (4) (2005) 847–864.
[9] Y. Xia, H. Hao, G. Zanardo, A. Deeks, Long term vibration monitoring of an RC slab: temperature and humidity effect, Eng. Struct. 28 (3) (2006) 441–452.
[10] Y. Xia, B. Chen, S. Weng, Y.-Q. Ni, Y.-L. Xu, Temperature effect on vibration properties of civil structures: a literature review and case studies, J. Civ. Struct. Health Monit. 2 (1) (2012) 29–46.
[11] M. Huang, Y. Lei, S. Cheng, Damage identification of bridge structure considering temperature variations based on particle swarm optimization-cuckoo search algorithm, Adv. Struct. Eng. 22 (15) (2019) 3262–3276.
[12] Z. Ding, K. Fu, W. Deng, J. Li, L. Zhongrong, A modified artificial bee colony algorithm for structural damage identification under varying temperature based on a novel objective function, Appl. Math. Model. 88 (2020) 122–141.
[13] M. Gonen, Analyzing Receiver Operating Characteristic Curves with SAS, SAS publishing, 2007.
[14] V. Giglioni, E. García-Macías, I. Venanzi, L. Ierimonti, F. Ubertini, The use of receiver operating characteristic curves and precision-versus-recall curves as performance metrics in unsupervised structural damage classification under changing environment, Eng. Struct. 246 (2021) 113029.
[15] Y. Xia, H. Hao, J.M. Brownjohn, P.-Q. Xia, Damage identification of structures with uncertain frequency and mode shape data, Earthq. Eng. Struct. Dyn. 31 (5) (2002) 1053–1066.
[16] Z. Ding, J. Li, H. Hao, Z.-R. Lu, Structural damage identification with uncertain modelling error and measurement noise by clustering based tree seeds algorithm, Eng. Struct. 185 (2019) 301–314.
[17] F.L. Wang, T.H. Chan, D.P. Thambiratnam, A.C. Tan, C.J. Cowled, Correlation-based damage detection for complicated truss bridges using multi-layer genetic algorithm, Adv. Struct. Eng. 15 (5) (2012) 693–706.
[18] T. Vo-Duy, V. Ho-Huu, H. Dang-Trung, T. Nguyen-Thoi, A two-step approach for damage detection in laminated composite structures using modal strain energy method and an improved differential evolution algorithm, Compos. Struct. 147 (2016) 42–53.
[19] F. Shabbir, M.I. Khan, N. Ahmad, M.F. Tahir, N. Ejaz, J. Hussain, Structural damage detection with different objective functions in noisy conditions using an evolutionary algorithm, Appl. Sci. 7 (12) (2017) 1245.
[20] M. Jahangiri, M. Najafgholipour, S. Dehghan, M. Hadianfard, The efficiency of a novel identification method for structural damage assessment using the first vibration mode data, J. Sound Vib. 458 (2019) 1–16.
[21] M. Jahangiri, M.A. Hadianfard, Vibration-based structural health monitoring using symbiotic organism search based on an improved objective function, J. Civ. Struct. Health Monit. 9 (5) (2019) 741–755.
[22] J. Humar, Dynamics of Structures, CRC Press, 2012.
[23] A.K. Chopra, Dynamics of structures. theory and applications to, Earthq. Eng. (2017).
[24] D.-C. Du, H.-H. Vinh, V.-D. Trung, N.-T. Hong Quyen, N.-T. Trung, Efficiency of jaya algorithm for solving the optimization-based structural damage identification problem based on a hybrid objective function, Eng. Optim. 50 (8) (2018) 1233–1251.
[25] M. Jahangiri, M.A. Hadianfard, M.A. Najafgholipour, M. Jahangiri, A reliability-based sieve technique: A novel multistage probabilistic methodology for the damage assessment of structures, Eng. Struct. 226, 111359.
[26] T. Fawcett, An introduction to ROC analysis, Pattern Recognit. Lett. 27 (8) (2006) 861–874.